Accepted Manuscript

Magnetoelectric coupling in strained strontium titanate and Metglas based magnetoelectric trilayer

S. Vivek, P. Geetha, K.V. Saravanan, S.K. Ajith, C.S. Chitralekha, K. Sudheendran, M.R. Anantharaman, S.S. Nair

PII: S0925-8388(19)30929-6

DOI: https://doi.org/10.1016/j.jallcom.2019.03.122

Reference: JALCOM 49886

To appear in: *Journal of Alloys and Compounds*

Received Date: 8 March 2018

Revised Date: 12 November 2018

Accepted Date: 6 March 2019

Please cite this article as: S. Vivek, P. Geetha, K.V. Saravanan, S.K. Ajith, C.S. Chitralekha, K. Sudheendran, M.R. Anantharaman, S.S. Nair, Magnetoelectric coupling in strained strontium titanate and Metglas based magnetoelectric trilayer, *Journal of Alloys and Compounds* (2019), doi: https://doi.org/10.1016/j.jallcom.2019.03.122.

Magnetoelectric Coupling in Strained Strontium Titanate and Metglas based MagnetoelectricTrilayer

S Vivek[a], P Geetha[b], K V Saravanan[c,d], S K Ajith[a], C S Chitralekha[a], K Sudheendran[e,f], M R Anantharaman[b#], S SNair[a,c#]

[a]Department of Physics, Central University of Kerala, Kasaragod, 671316, India
[b]Department of Physics, Cochin University of Science and Technology, Cochin 682022, India
[c]Departmento de Física and I3N, Universidade de Aveiro, 3810-193 Portugal
[d]Department of Physics, Central University of Tamil Nadu, Tiruvarur, Tamilnadu, 610 004, India
[e]Department of Physics, Sree Kerala Varma College, Thrissur, Kerala, India
[f]Department of Physics, University of Puerto Rico at Rio Piedras, San Juan, PR 00936-8377, U.S.A

E-mail: swapna.s.nair@gmail.com

Abstract: Direct magneto electric coupling is observed with a magnetoelectric coupling coefficient (MECC) of 806 mV cm^{-1} Oe^{-1} at 750 Hz in strontium titanate (STO) - Metglas - strontium titanate (STO-Metglas-STO) trilayer thin films with a total thickness of 600 nm. The piezoelectricity in the strained STO layer, which is otherwise a paraelectric material, enabled the sandwiched magneto electric structure to exhibit a fair sub resonant magneto electric coupling. Theoretical models proposed by Bichurin *et al*. and Hanyasan *et al*. are employed to calculate the values of MECC at sub resonant condition for the system, which is noted as 853 mV cm^{-1} Oe^{-1}. The frequency dependence of MECC coefficient is also calculated and the resonance frequency is estimated as 706 Hz.

Keywords: nanostructured materials, thin films, composite materials, magnetostriction, piezoelectricity, electrostrition.

1. Introduction

Multiferroics are multifunctional materials with the coexistence of two or more ferroic orders. Ferroic orders can be ferroelectric, ferro/antiferromagnetic, ferroelastic and ferrotorroidic. In magnetoelectric multiferroics, both magnetic and ferroelectric states exist together and they are coupled to each other. Generally, it can be classified into single phase and composite magnetoelectric multiferroics. Single phase magnetoelectric materials have displayed many interesting physical phenomena like magnetism driven ferroelectricity [1], observation of skyrmions [2], magnetization switching using electric field at room temperature [3] etc. But for device fabrication, magnetoelectric composite materials are preferred due to their superior magnetoelectric coupling compared to their single phase counterparts [4]. The magnetoelectric characteristics of magnetoelectric composites are product tensor property. Because of the strong mechanical coupling between ferromagnetic and ferroelectric layers, strain induced via magnetostriction in the ferromagnetic layer changes piezoelectric properties of the ferroelectric/piezoelectric layer [5]. It is important to study different magneoelectric systems to understand the coupling mechanisms better.

Piezoelectrics are materials that can convert mechanical energy into electrical energy and vice versa. These materials are actively being researched since it finds applications in the field of energy harvesting, microsensors, actuators, robotics, etc [6]. Realization of a piezoelectric FET based on single ZnO nanowire has opened up a new arena of research [7]. Such coupling of material properties to strain can give an additional control over the electronic transport. The piezoelectric material used in this study is STO. It is one of the widely investigated materials due to the rich diversity of physical phenomena displayed by it like incipient ferroelectricity [8], enhancement of dielectric constant at cryogenic temperature [9], low temperature phase transition [10], superconductivity [11], etc. It's high dielectric constant, high thermal stability and low microwave losses find applications in tunable microwave devices [12][13]. The incipient ferroelectric state of pure STO can be easily disturbed by

outside factors like strain [14], electric field [15], chemical substitution [16], oxygen isotope exchange [17], etc. Haeni *et al*. have grown STO on $DyScO_3$ substrate with a tensile lattice mismatch of + 1% and observed ferroelectricity up to 293 K [18]. Sun *et al*. have computed piezoelectric properties of STO as a function of misfit strain. They used a linear thermodynamical model and predicted that the in-plane misfit strain in STO can produce piezoelectric coefficients that are comparable to the well-established lead-based piezoceramics [19]. Piezoelectricity due to non-homogenous strain is reported in STO, in which the local strain gradients polarized the domain walls of STO. Kholkin *et al*. reported room temperature piezoelectricity due to surface strain gradients [20].

In this work, we have adopted strained STO as the piezoelectric layer and cobalt rich Metglas (Commercially available Metglas 2714A) as the magnetic layer. It has high permeability compared with the commonly used magnetic materials employed in the fabrication of magnetoelectric composites. Dong *et al*. used a highly permeable FeBSiC alloy to obtain very high MECC value of 22 V/cm Oe [21].

To the best of our knowledge, this is the first time strained STO is used as the piezoelectric layer in a magnetoelectric system. In this work, we report the fabrication of STO-Metglas-STO trilayer thin film structure. The ferromagnetic, ferroelectric and magnetoelectric properties of the trilayer structure are investigated.

2. Materials and Methods

Sol-gel spin coating method was used for the preparation of STO film on Si/SiO_2; Ti/Pt substrate. STO sol was prepared using precursors strontium nitrate, titanium isopropoxide and 2-methoxy ethanol. The prepared sol was homogenized after thorough stirring for 6 hours and ultrasonicated and aged for 72 hours. A programmable spin coater was used to deposit the homogenized sol on ultrasonically and chemically cleaned Pt coated Si substrates at a speed of 6000 rpm. As prepared STO film was pyrolyzed under oxygen atmosphere at 250°C for 30 minutes and later annealed at 700°C for 1 hour. Thermal evaporation technique (at room temperature) was used to deposit commercially available Metglas 2714A alloy ribbon (cobalt rich) onto the already deposited STO layer at a pressure of 10^{-6}Torr. Sol-gel spin coating was again employed to deposit a STO layer on top of the Metglas layer. The multilayer films were etched out at the corner with 5% HCl+HF solution so as to open the Pt electrode. Gold was sputtered on top of the surface STO layer as the top electrode, and lead contacts were soldered for the magnetoelectric coupling studies. The multilayer on Si/Pt substrate was grinded to ~120 μm (along the thickness direction) using a disk grinder followed by polishing with polishing papers. Cantilevers of the size 3 mm × 15 mm were cut using a dicer.

The crystallographic phases of the multilayer were analyzed using Rigaku D Max X Ray diffractometer (copper Kα = 1.5404 Å). Lattice strain was calculated after evaluating the full width at half maxima (FWHM) of the (200) lattice plane. The morphological characterization was done using scanning electron microscope (HR-SEM-SE/EDS: SEM marca Hitachi, model SU-70 e EDS marcaBruker, modelo QUANTAX 400). The morphology of the film (SEM), its composition (EDS) and cross section (CS SEM) was recorded. The films were analyzed for probing into the particle size and lattice strain through high resolution transmission electron microscopy (HR–TEM200–SE/EDS: HR-(EF) TEM marca JEOL, model 2200FS and EDS marca Oxford, model INCA Energy TEM 250). The magnetic properties of the thin films were probed using Quantum Design MPMS 5XL SQUID Magnetometer. Ferroelectric hysteresis loops were traced using Radiant RT 66B ferroelectric tester. The magneto electric coupling studies were carried out using a setup that consisted of an electromagnet and a pair of Helmholtz coils that generate the dc bias field and the ac driving fields respectively, extended with a lock-in amplifier (Model: DSP 7270). The frequency dependence was studied at 28 Oe dc magnetic field, ~10 Oe ac modulating field (from 500 Hz to 1.5 kHz). LabVIEW automated system was used for data acquisition. The off-resonant MECC value was determined at room temperature as a function of the biasing dc magnetic field by measuring the ME voltage developed when a low frequency (500 Hz)

magnetic field with an amplitude of ~ 10 Oe (the field will slightly change with the change in applied frequency) was applied to the thin film cantilevers. The low modulation frequency of 500 Hz was chosen as the starting frequency to avoid resonance effects. Frequencies less than 500 Hz were not applied in order to avoid the interfacial polarization effects and high losses usually present at very low frequencies. Frequency dependence was studied from 500 Hz to 1.5 kHz range [22].

3. Results and Discussion

Figure 1 (a) represents the XRD pattern of STO-Metglas-STO trilayer thin film. Peaks corresponding to cubic STO are indexed in Fig. 1(a) (JCPDS card no. 35-0734). Structural analysis showed that the STO is in perovskite structure with a lattice constant of 0.3896 nm. The XRD peak observed at 2θ = 40° is a doublet and hence the peaks were deconvoluted using Lorentzian fitting as shown in Figure 1 (b). Figure 2 (a) shows the cross sectional SEM image of the trilayer film. The thickness of individual layers is found to be 180 nm, 240 nm and 180 nm for the top STO, middle Metglas and bottom STO layers respectively. HRTEM image of the Metglas layer (recorded before the deposition of the top layer) is shown in Figure 2 (b), in which (110) plane of α-Fe and (111) plane of β-Co is indexed which shows nanocrystallisation upon annealing whose signatures were not observed in XRD, due to small and discontinuous grains.

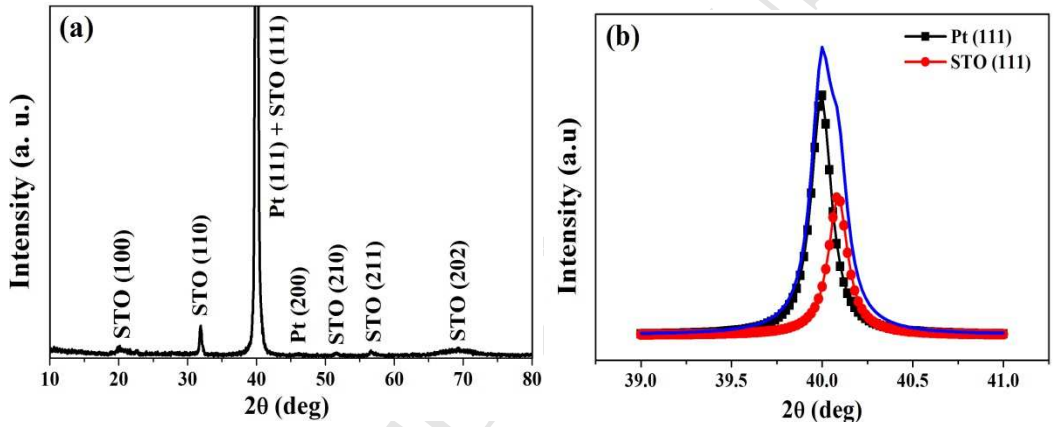

Figure 1.(a) XRD of STO-Metglas-STO trilayer and (b) enlarged

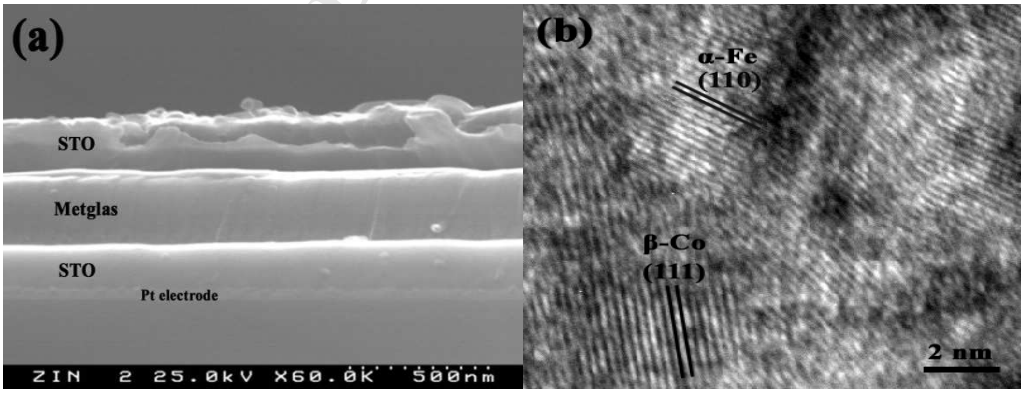

Figure 2. (a) Cross sectional SEM of STO-Metglas-STO trilayer and (b) HRTEM image of Metglas middle layer

In the present investigation Si/SiO_2; Ti/Pt substrate was used. A (111) textured Pt foil was used to deposit the Pt layer and was further annealed to make it more crystalline. The lattice constant of fcc platinum (0.3920 nm) is close to the lattice constant of the strain free strontium titanate (0.3904 nm). The growth of (111) textured STO film, as observed from

XRD indicates that the nucleation and crystal growth of STO layer started on the surface of Pt layer, which can result in a compressive strain on STO film. Compared to polycrystalline STO, both (110) and (111) peaks of STO film are shifted to lower 2θ values, which can be attributed to compressive strain. Many studies on strained STO used $DyScO_3$ substrate with a lattice mismatch of 1% [18][23]. The possibility of strain relaxation is even less in this case since the biaxial strain is only 0.2%. This biaxial strain is mainly responsible for its piezoelectric nature [19].

The piezoelectric properties of the trilayer thin film were investigated using Piezoresponse Force Microscope (PFM). Figure 3 (a) and 3 (b) represents the piezoresponse of the amplitude and phase images of the bottom STO layer before the deposition of the middle and top layers. The dark and bright contrast in Figure 3 (b) shows the anti-parallel orientation of the piezodomains. Figure 3 (c) and 3 (d) represent the bias field dependence of the PFM amplitude and the corresponding phase respectively. PFM amplitude shows a well-shaped butterfly loop and the corresponding phase indicates a polarization switching. The horizontal shift observed in these loops can be attributed to the strain in the STO lattice [24]. The piezoelectric coefficient of bottom STO was calculated from the piezoresponse and an average value of 22 pm/V was obtained for a biasing voltage of +1 V. This value is less than the ferroelectric KNN (45 pm/V) [25] but greater than $Ba(Ti, Zr)O_3$ (9 pm/V) [26] and $SrBi_2Ta_2O_9$ (17 pm/V) [27] thin films made by sol-gel/spin-coating method. The top STO layer is only slightly piezoelectric with a d_{33} value of 1.5 pm/V. This is mainly due to the presence of middle Metglas layer, which confines the strain to the bottom STO layer. From HRTEM images, it is observed that the middle Metglas layer is partially crystallized. G. Buttino *et al*. have observed nanocrystalline phase of Metglas 2714A when it is heated above its crystallization temperature of 550°C [28][29]. This partial crystallization of the Metglas layer at the interface could possibly create strain gradients, which may further increase the piezoelectricity [20].

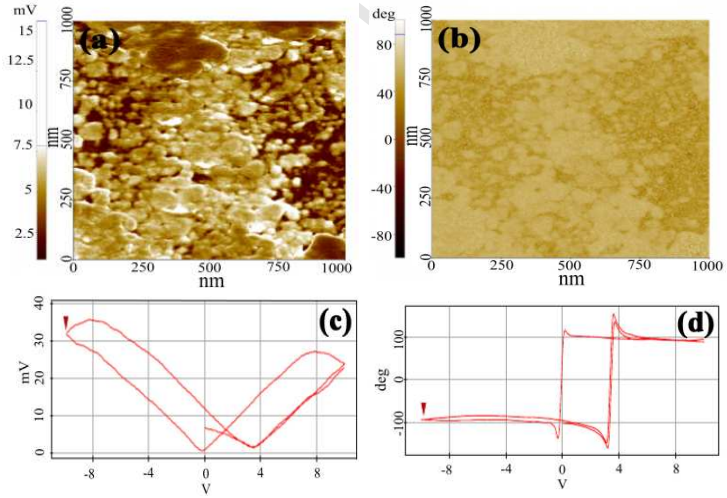

Figure 3. (a) Piezoresponse of the amplitude and (b) the corresponding phase of the bottom STO layer before the deposition of the middle and top layers. Bias field dependence of the PFM amplitude (c) and the corresponding phase (d).

Magnetic hysteresis loop for the STO-Metglas-STO trilayer is shown in figure 4 from which the coercivity is found to be 69 Oe and saturation magnetization as 832 emu/cc. High saturation magnetization and low coercivity of Metglas is maintained in the trilayer with a high squareness ratio (0.82).

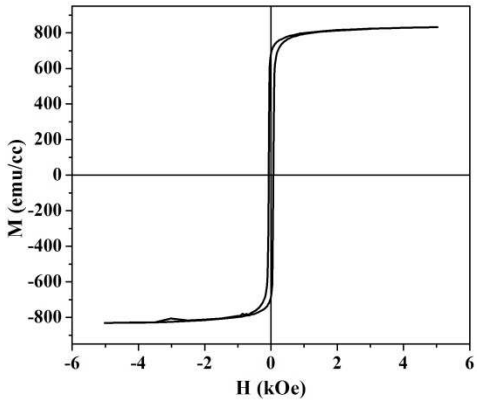

Figure 4.M-H loop of the STO-Metglas-STO trilayer.

Dc magnetic field dependence of MECC is studied in the trilayer thin film. A maximum MECC of 806 mV cm^{-1} Oe^{-1} is recorded for a dc biasing field of 28 Oe, which is shown in figure 5 (a). The frequency dependence of the magnetoelectric coupling at a dc magnetic field of 28 Oe showed a sharp resonance peak at 753 Hz with an MECC of 20 V cm^{-1} Oe^{-1} which is depicted in figure 5 (b). When the driving frequency equals the acoustic resonance of the cantilever, a sudden increase in the MECC value was noted, which is depicted in the figure. The MECC value at resonant frequency is about 25 times larger compared to its sub-resonant MECC value of 806 mV cm^{-1} Oe^{-1}. At higher fields, the MECC values approaches zero due to saturation of the magnetostriction, which in turn reduces the piezomagnetic coupling term (q_{ij}^m) to zero and also due to the weakening of ac magnetomechanical coupling. We calculated the magnetoelectric coupling coefficient using the model proposed by Bichurin *et al*. [30].

$$\alpha_{E,31} = \frac{-kv(v-1)d_{31}^P(q_{11}^m + q_{21}^m)}{(s_{11}^m + s_{12}^m)\varepsilon_{33}^{T,P}kv + (s_{11}^P + s_{12}^P)\varepsilon_{33}^{T,P}(1-v) - 2(d_{31}^P)^2k(1-v)} \quad \ldots (1)$$

Where k is the interface coupling parameter, which is assumed to be ideal (k = 1), v is the volume fraction for the piezoelectric material used and $d_{31}^P$is the piezoelectric constant for the strained STO. q_{ij}^m is the longitudinal piezomagnetic coefficient for the magnetic layer. s_{ij}^m and s_{ij}^p are the components of compliance tensors for the magnetic and piezoelectric layers. $\varepsilon_{33}^{T,P}$is the dielectric constant of the piezoelectric layer. The calculated value, 853 mV cm^{-1} Oe^{-1}, is close to the observed magnetoelectric coupling coefficient of 806 mV cm^{-1} Oe^{-1}. The piezomagnetic coefficient (q_{ij}^m) will increase due to the high permeability of the magnetic layer. From previous reports, a highly permeable magnetic layer plays the key role for enhancing the MECC value instead of a highly magnetostrictive magnetic layer. The low piezoelectric coefficient of STO is compensated by the high piezomagnetic constant of the magnetic layer, which resulted in the observed MECC value. According to the magnetoelectric equivalent model proposed by Zhai *et al.*, the high magnetostriction of the middle magnetic layer results in a large strain in the upper and lower piezoelectric layers which could enhance the magnetoelectric coupling [31]. The magnetostriction value in the as-received Metglas 2714A is nearly zero. It is observed that annealing near the crystallization temperature enhances the magnestostriction value of Metglas layer [28]. It is evident from HRTM image that bcc phase of Fe and fcc phase of Co is formed. This coexistence of both the bcc and fcc phase may have contributed to the enhanced magnetostriction as in the case of the Co rich magnetic alloy system $Co_{1-x}Fe_x$ [32]. At the interface between STO and Metglas,

surface charges may increase due to the high dielectric constant of STO. The inter layer magnetoelectric coupling, which is proportional to the surface charges is increased at the interface which may also have contributed to the observed MECC value [33].

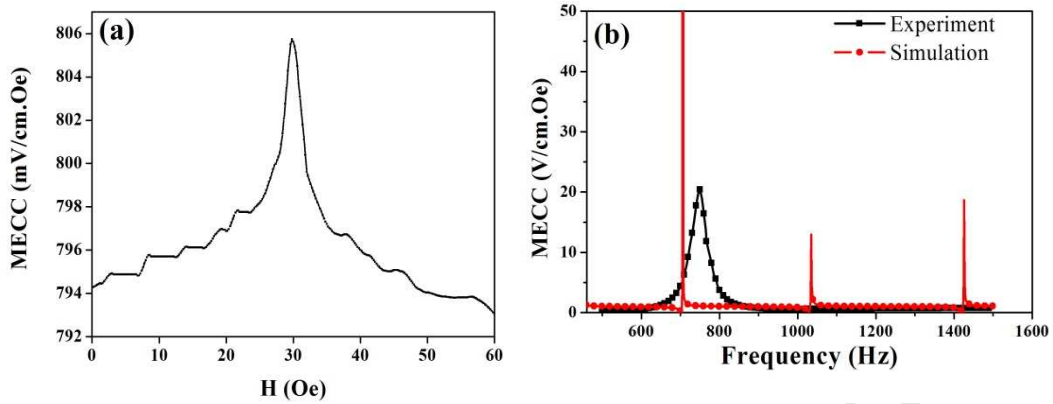

Figure 5. (a) MECC variation with magnetic field and (b) MECC vs. frequency graph for STO-Metglas-STO trilayer

Based on the model proposed by Hanyasan *et al.* [34], we have calculated the resonance frequency for the magnetoelectric laminate structure. Compared to previous models which consider interactions only along the longitudinal direction, this model include the interactions along the thickness of the multilayers. Based on that model, the MECC with respect to frequency can be written as,

$$\alpha_{ME}(\omega) = -\frac{q_{11}d_{11}}{Sp_{11}\varepsilon_{11}}\frac{h_p}{h_p+h_m}\frac{\Delta_{0I}}{\Delta_{0II}} \ldots (2)$$

Where $\Delta_{0I} = \frac{\gamma_0}{\gamma_0+1}\frac{\tan(\lambda_T L)}{\lambda_T L} - \frac{3}{2}\frac{\gamma_1}{\gamma_2+1}\Delta_o(\lambda_B L)$,

$$\Delta_{0II} = 1 - K_1^2 + K_1^2\frac{1}{\gamma_0+1}\frac{\tan(\lambda_T L)}{\lambda_T L} + \frac{3}{2}K_1^2\frac{\gamma_1}{\gamma_2+1}\Delta_o(\lambda_B L),$$

$$\Delta_o(\lambda_B L) = \frac{\sinh(\lambda_B L)}{\sinh(\lambda_B L)\cos(\lambda_B L)+\sin(\lambda_B L)\cosh(\lambda_B L)}\frac{\sin(\lambda_B L)}{\lambda_B L}.$$

$$\lambda_T = \sqrt{\frac{\omega^2\rho}{A}}, \qquad \lambda_B = \sqrt[4]{\frac{\omega^2\rho}{D}},$$

Where, $A = \sum_{k=1}^{N_P}\frac{h_{kP}}{S_{P11}^{(k)}} + \sum_{k=1}^{N_M}\frac{h_{kM}}{S_{M11}^{(k)}}$,

$$D = \sum_{k=1}^{N_P}\frac{1}{3S_{P11}^{(k)}}\left[\left(Z_k^P\right)^3 - \left(Z_{k-1}^P\right)^3\right] + \sum_{k=1}^{N_P}\frac{1}{3S_{M11}^{(k)}}\left[\left(Z_k^M\right)^3 - \left(Z_{k-1}^M\right)^3\right],$$

$$\rho = \sum_{k=1}^{N_P} h_{kP}\rho_{kP} + \sum_{k=1}^{N_M} h_{kM}\rho_{kM}$$

$$\gamma_0 = \frac{S_{P11}h_m}{S_{M11}h_p},\ \gamma_1 = \frac{S_{P11}}{S_{M11}}\left[\frac{h_m}{h_p}\right]^2,\ \gamma_2 = \frac{S_{P11}}{S_{M11}}\left[\frac{h_m}{h_p}\right]^3,\ K_1^2 = \frac{d_{11}^2}{S_{P11}\varepsilon_{11}}.$$

Where L is the length of the thin film cantilever, N_P and N_M are the number of piezoelectric and magnetic layers. h_{kP} and h_{kM} are the are the thickness of the piezoelectric and magnetic k^{th} layers. D is the sum of dielectric displacement of every layer, including that of substrate. Z values corresponds to the thickness of the respective layers, which are $Z_0 = 0$, $Z_1 = h_{Si}$ (thickness of the Si layer in the substrate), $Z_2 = Z_1 + h_{SiO_2}$ (h_{SiO_2} is the thickness of the SiO_2 layer in the substrate), $Z_3 = Z_2 + h_{ti}$ (h_{ti} is the thickness of the titanium layer in the substrate),

$Z_4 = Z_3 + h_P/2$, $Z_5 = Z_4 + h_M$, $Z_6 = Z_5 + h_P/2$. For calculations, we have taken the same material parameters (d_{31}^P, q_{ij}^m, s_{ij}^m, s_{ij}^P and $\varepsilon_{33}^{T,P}$) as in the previous section. Total thickness of the magnetoelectric structure includes that of Si, SiO_2, Pt and Ti, which is considered in this calculation. Figure 5 (b) shows the MECC vs. frequency for both the experimental and calculated values. The observed resonance peak of MECC is at 750 Hz and the calculated value is 706 Hz. The model that is used to calculate the MECC value assumed that between layers, the strains are small and the layers are perfectly bonded. But as discussed previously, there may be strain in the layers and the layers are not perfectly bonded, which may be the reason for the difference in observed and calculated resonant frequencies. The calculated resonant frequencies had peaks at 1036 Hz and 1430 Hz, which were not observed. This is due to low intensity (1: 34) of these peaks compared to the peak at resonance.

4. Conclusion

The STO-Metglas-STO trilayer cantilevers were fabricated on an Si/SiO_2; Ti/Pt substrate which exhibited a sub resonant MECC of 806 mV cm^{-1} Oe^{-1} at 750 Hz. From the XRD studies, a change in the preferred orientation of STO layer and a shift in the 2θ values of major peaks of STO layer were observed, which may be due to strain in the STO layer. Strained STO layer became piezoelectric, which is confirmed from PFM studies. From the HRTEM image, it is observed that the Metglas layer is partially crystallized. Magnetostriction may increase due to this partial crystallization. So the enhanced magnetoelectric coupling between the piezoelectric STO layer and magnetostrictive Metglas layer may be the reason for the observed MECC value. Based on the model proposed by Hanyasan *et al*., the MECC at sub-resonant frequency and the resonant frequencies were calculated as 853 mV cm^{-1} Oe^{-1} and 706 Hz respectively. The experimental results showed a discrepancy of 5.7% error for MECC coefficient and 6% error for resonant frequency, which may be due to the strains and imperfect bonding between the layers.

Acknowledgments

SSN acknowledges UGC (F.No.201/2013), DST (YSS/2014/000431) and DBT (6292-P52/RGCB/PMD/DBT/RPKT/2015) for the financial support. SSN also acknowledges Prof. Nikolai A. Sobolev Andrei L. Kholkin and Igor Bdkin, CICECO, Universidade de Aveiro, for extending necessary infrastructure and lab facilities. The team also acknowledges Prof. GlebKakazei, Universidade do Porto for magnetic measurements (SQUID). GP acknowledges UGC, India for providing financial assistance in the form of RFSMS fellowship (No.F4-3/2006(BSR)/8-3/2007(BSR)). MRA acknowledges DAE-BRNS for funding provided in the form of a project (No: 2011/34/7/BRNS/0596).

References

[1] T. Kimura, Magnetoelectric Hexaferrites, Annu. Rev. Condens. Matter Phys. 3 (2012) 93–110. doi:10.1146/annurev-conmatphys-020911-125101.

[2] S. Seki, X.Z. Yu, S. Ishiwata, Y. Tokura, Observation of Skyrmions in a Multiferroic Material, Science (80-.). 336 (2012) 198 LP-201. http://science.sciencemag.org/content/336/6078/198.abstract.

[3] J.T. Heron, J.L. Bosse, Q. He, Y. Gao, M. Trassin, L. Ye, J.D. Clarkson, C. Wang, J. Liu, S. Salahuddin, D.C. Ralph, D.G. Schlom, J. Íñiguez, B.D. Huey, R. Ramesh, Deterministic switching of ferromagnetism at room temperature using an electric field, Nature. 516 (2014) 370–373. doi:10.1038/nature14004.

[4] W. Prellier, M.P. Singh, P. Murugavel, The single-phase multiferroic oxides: from bulk to thin film, J. Phys. Condens. Matter. 17 (2005) R803. http://stacks.iop.org/0953-8984/17/i=30/a=R01.

[5] C. Nan, M.I. Bichurin, S. Dong, D. Viehland, G. Srinivasan, Multiferroic magnetoelectric composites : Historical perspective , status , and future directions, J. Appl. Phys. 103 (n.d.). http://cat.inist.fr/?aModele=afficheN&cpsidt=20179615.

[6] G.J. and W.C. and Y. Zheng, A review of recent ab initio studies on strain-tunable conductivity in tunnel junctions with piezoelectric, ferroelectric and multiferroic barriers, Semicond. Sci. Technol. 32 (2017) 83006. http://stacks.iop.org/0268-1242/32/i=8/a=083006.

[7] X. Wang, J. Zhou, J. Song, J. Liu, N. Xu, Z.L. Wang, Piezoelectric Field Effect Transistor and Nanoforce Sensor Based on a Single ZnO Nanowire, Nano Lett. 6 (2006) 2768–2772. doi:10.1021/nl061802g.

[8] W. Zhong, D. Vanderbilt, Effect of quantum fluctuations on structural phase transitions in $SrTiO_3$ and $BaTiO_3$, Phys. Rev. B. 53 (1996) 5047–5050. https://link.aps.org/doi/10.1103/PhysRevB.53.5047.

[9] K.A. Müller, H. Burkard, $SrTiO_3$: An intrinsic quantum paraelectric below 4 K, Phys. Rev. B. 19 (1979) 3593–3602. https://link.aps.org/doi/10.1103/PhysRevB.19.3593.

[10] P.A. Fleury, J.F. Scott, J.M. Worlock, Soft Phonon Modes and the 110° K Phase Transition in $SrTiO_3$, Phys. Rev. Lett. 21 (1968) 16–19. https://link.aps.org/doi/10.1103/PhysRevLett.21.16.

[11] J.F. Schooley, W.R. Hosler, M.L. Cohen, Superconductivity in Semiconducting $SrTiO_3$, Phys. Rev. Lett. 12 (1964) 474–475. https://link.aps.org/doi/10.1103/PhysRevLett.12.474.

[12] J. Krupka, R.G. Geyer, M. Kuhn, J.H. Hinken, Dielectric properties of single crystals of Al_2O_3 , $LaAlO_3$, $NdGaO_3$, $SrTiO_3$, and MgO at cryogenic temperatures, IEEE Trans. Microw. Theory Tech. 42 (1994) 1886–1890. doi:10.1109/22.320769.

[13] G. Rupprecht, R.O. Bell, Microwave Losses in Strontium Titanate above the Phase Transition, Phys. Rev. 125 (1962) 1915–1920. https://link.aps.org/doi/10.1103/PhysRev.125.1915.

[14] N.A. Pertsev, A.K. Tagantsev, N. Setter, Phase transitions and strain-induced ferroelectricity in $SrTiO_3$ epitaxial thin films, Phys. Rev. B. 61 (2000) R825–R829. http://link.aps.org/doi/10.1103/PhysRevB.61.R825.

[15] P.A. Fleury, J.M. Worlock, Electric-Field-Induced Raman Scattering in $SrTiO_3$ and $KTaO_3$, Phys. Rev. 174 (1968) 613–623. http://link.aps.org/doi/10.1103/PhysRev.174.613.

[16] J.G. Bednorz, K.A. Müller, $Sr_{1-x}Ca_xTiO_3$: An XY Quantum Ferroelectric with Transition to Randomness, Phys. Rev. Lett. 52 (1984) 2289.

[17] M. Itoh, R. Wang, Y. Inaguma, T. Yamaguchi, Y.-J. Shan, T. Nakamura, Ferroelectricity Induced by Oxygen Isotope Exchange in Strontium Titanate Perovskite, Phys. Rev. Lett. 82 (1999) 3540–3543. http://link.aps.org/doi/10.1103/PhysRevLett.82.3540.

[18] J.H. Haeni, P. Irvin, W. Chang, R. Uecker, P. Reiche, Y.L. Li, S. Choudhury, W. Tian, M.E. Hawley, B. Craigo, A.K. Tagantsev, X.Q. Pan, S.K. Streiffer, L.Q. Chen, S.W.

Kirchoefer, J. Levy, D.G. Schlom, Room-temperature ferroelectricity in strained SrTiO3, Nature. 430 (2004) 758–761. http://dx.doi.org/10.1038/nature02773.

[19] F. Sun, H. Khassaf, S.P. Alpay, Strain engineering of piezoelectric properties of strontium titanate thin films, J. Mater. Sci. 49 (n.d.) 5978–5985. http://cat.inist.fr/?aModele=afficheN&cpsidt=28450190 (accessed September 28, 2016).

[20] A. Kholkin, I. Bdikin, T. Ostapchuk, J. Petzelt, A. Kholkin, I. Bdikin, T. Ostapchuk, J. Petzelt, Room temperature surface piezoelectricity in $SrTiO_3$ ceramics via piezoresponse force microscopy, 222905 (2015) 2006–2009. doi:10.1063/1.3037220.

[21] S. Dong, J. Zhai, J. Li, D. Viehland, Near-ideal magnetoelectricity in high-permeability magnetostrictive/piezofiber laminates with a (2-1) connectivity, Appl. Phys. Lett. 89 (2006) 252904. doi:10.1063/1.2420772.

[22] B.M. Kulwicki, R. Tsu, Barium strontium titanate (BST) thin films using boron, (2001).

[23] Y.L. Li, S. Choudhury, J.H. Haeni, M.D. Biegalski, A. Vasudevarao, A. Sharan, H.Z. Ma, J. Levy, V. Gopalan, S. Trolier-McKinstry, D.G. Schlom, Q.X. Jia, L.Q. Chen, Phase transitions and domain structures in strained pseudocubic (100) $SrTiO_3$ thin films, Phys. Rev. B. 73 (2006) 184112. https://link.aps.org/doi/10.1103/PhysRevB.73.184112.

[24] Y.S. and S.W. and M.K. and H.Y. and K. Matsushige, Investigation of Nonswitching Regions in Ferroelectric Thin Films Using Scanning Force Microscopy, Jpn. J. Appl. Phys. 39 (2000) 3799. http://stacks.iop.org/1347-4065/39/i=6S/a=3799.

[25] Q. Yu, J.-F. Li, W. Sun, Z. Zhou, Y. Xu, Z.-K. Xie, F.-P. Lai, Q.-M. Wang, Electrical properties of $K_{0.5}Na_{0.5}NbO_3$ thin films grown on Nb:$SrTiO_3$ single-crystalline substrates with different crystallographic orientations, J. Appl. Phys. 113 (2013) 24101. doi:10.1063/1.4773542.

[26] K.T. and K.S. and K.N. and T.M. and K. Kato, Microstructure Control and Dielectric/Piezoelectric Properties of Alkoxy-Derived Ba(Ti,Zr)O_3 Thin Films, Jpn. J. Appl. Phys. 44 (2005) 6885. http://stacks.iop.org/1347-4065/44/i=9S/a=6885.

[27] A.L. Kholkin, E.K. Akdogan, A. Safari, P.-F. Chauvy, N. Setter, Characterization of the effective electrostriction coefficients in ferroelectric thin films, J. Appl. Phys. 89 (2001) 8066–8073. doi:10.1063/1.1371002.

[28] G. Buttino, A. Cecchetti, M. Poppi, Magnetic softening and nanocrystallization in amorphous Co-rich alloys, J. Magn. Magn. Mater. 172 (1997) 147–152. doi:https://doi.org/10.1016/S0304-8853(97)00126-1.

[29] C.S. Chitra Lekha, A.S. Kumar, S. Vivek, M.R. Anantharaman, K. Venkata Saravanan, S.S. Nair, Strain induced giant magnetoelectric coupling in KNN/Metglas/KNN sandwich multilayers, Appl. Phys. Lett. 110 (2017) 12901. doi:10.1063/1.4973450.

[30] M.I. Bichurin, V.M. Petrov, G. Srinivasan, Theory of low-frequency magnetoelectric effects in ferromagnetic-ferroelectric layered composites, J. Appl. Phys. 92 (2002) 7681–7683. doi:10.1063/1.1522834.

[31] J. Zhai, S. Dong, Z. Xing, J. Li, D. Viehland, Giant magnetoelectric effect in Metglas/polyvinylidene-fluoride laminates, Appl. Phys. Lett. 89 (2006) 083507.

doi:10.1063/1.2337996.

[32] D. Hunter, W. Osborn, K. Wang, N. Kazantseva, J. Hattrick-Simpers, R. Suchoski, R. Takahashi, M.L. Young, A. Mehta, L.A. Bendersky, S.E. Lofland, M. Wuttig, I. Takeuchi, Giant magnetostriction in annealed $Co_{1-x}Fe_x$ thin-films, Nat Commun. 2 (2011) 518. http://dx.doi.org/10.1038/ncomms1529.

[33] J.M. Rondinelli, M. Stengel, N.A. Spaldin, Carrier-mediated magnetoelectricity in complex oxide heterostructures, Nat Nano. 3 (2008) 46–50. http://dx.doi.org/10.1038/nnano.2007.412.

[34] D. Hasanyan, J. Gao, Y. Wang, R. Viswan, M. Li, Y. Shen, J. Li, D. Viehland, Theoretical and experimental investigation of magnetoelectric effect for bending-tension coupled modes in magnetostrictive-piezoelectric layered composites, J. Appl. Phys. 112 (2012) 13908. doi:10.1063/1.4732130.

Highlights

- Piezoelectricity in strained strontium titanate (STO) with a d_{33} value of 22 pm/V.
- First time employment of strained STO in magnetoelectric heterostructures.
- ME coupling coefficient of 806 mV cm^{-1} Oe^{-1}, Metglas being its magnetic component.
- Theoretical fitting is provided for the ME coupling effects for STO-Metglas-STO.